



ELSEVIER

Contents lists available at [ScienceDirect](https://www.sciencedirect.com)

Results in Control and Optimization

journal homepage: www.elsevier.com/locate/rico

Optimal PID controller for the DC-DC buck converter using the improved sine cosine algorithm

Norsyahidatul Farah Nanyan^a, Mohd Ashraf Ahmad^{a,*}, Baran Hekimoğlu^b

^a Faculty of Electrical and Electronics Engineering Technology, Universiti Malaysia Pahang Al-Sultan Abdullah, Pekan, Pahang 26600, Malaysia

^b Department of Electrical & Electronics Engineering, Batman University, Batman 72100 Turkey

ARTICLE INFO

Keywords:

Sine cosine algorithm
Improved sine cosine algorithm (ISCA)
Algorithm-based PID controller
DC-DC buck converter

ABSTRACT

This paper presents an improved Sine Cosine Algorithm (ISCA) towards optimization of a DC-DC buck converter with employment of the proportional-integral-derivative (PID) controller. Limitations of the conventional Sine Cosine Algorithm (SCA) was hereby overcome through two separate alterations which pioneered a synergized employment of nonlinear equation to instrumental mechanism in revising the average location. Primary alteration tackled the issue of local optima by proposed instrumental function towards revision of average location. Secondary alteration then coordinated disproportional exploration and exploitation phases of the conventional SCA by application of a nonlinear equation against the algorithm's decreasing position-updated mechanism. Robustness of the proposed ISCA-PID approach was studied against preceding algorithm-based PID for DC-DC buck converter with respect to their step response, statistics regarding the analyzed objective function, time-domain integral-error performance, reaction to frequency, and resistance to disturbance and parametric uncertainties. Generated findings subsequently uncovered overshadowing efficacy of the proposed method over its algorithmic predecessors towards exceptionally enhanced transitory response of the DC-DC buck converter.

1. Introduction

Volatility of a DC-DC buck converter fundamentally ensued its renowned implementation across vast industrial applications across differential fields of integrated technologies for generation of renewable energy [1], electricity-powered automobiles [2], automated devices [3], light-weighted electrical instruments [4] and as well as end user computing [5–10]. Robustness of the system is then capitalized its extensive power density, proficiency, affordability, agility, with being dependable towards particular operational specifications [11]. Categorized as a switched-mode power supply (SMPS), lateral setup of electronic elements including diodes, transistors, inductors and capacitors, thus, enabled the system's functionality towards voltage step-down [12]. Practical variants with the like of Sepic, Zeta, Cuk, Boost, Buck and Buck-Boost have also surfaced as among the types of contemporary DC-DC converters adopted towards instruments which demand transition of low DC voltage [11]. Nevertheless, obstacle rendering complications towards development of control blueprint within these converters was determined on the coordination of preferred output voltage under circumstances of unstable voltage input, weighed of included load and values of elements throughout the operating circuit. The desire to overcome such issue further propelled practical adaptation of numerous control mechanisms spanning wide extent of technical complexities.

* Corresponding author.

E-mail address: mashraf@ump.edu.my (M.A. Ahmad).

<https://doi.org/10.1016/j.rico.2023.100352>

Received 3 March 2023; Received in revised form 3 September 2023; Accepted 27 November 2023

Available online 28 November 2023

2666-7207/© 2023 The Author(s). Published by Elsevier B.V. This is an open access article under the CC BY-NC-ND license (<http://creativecommons.org/licenses/by-nc-nd/4.0/>).

Among others, the voltage-mode control was introduced as an initial control mechanism for such purpose [13]. Having observed a steady readjustment from the employed system across extended frequencies, outputs of the buck converter through implementation of voltage-mode control has, yet, accompanied deterioration from immense sensitivity of its loop gain to the least alteration in input voltage. With subsequent outlook by [14] proposed maneuvering of a DC-DC buck converter through Type-II and Type-III feedback compensators following installation of an error amplifier, the mechanism's simplistic structure then came with an unsatisfactory handling stability. Furthering the resolution was the introduction of advanced control blueprint called sliding mode control (SMC) which utilizes a disconnecting control signal to forcibly command system's transition in the cross-sectioned route to its regular maneuver for reshaped mobility [15]. While effective and instantaneous directory reactions were demonstrated through such approach, real-time employment of SMC then revealed several shortcomings in the form of fluctuations in switching frequency, existence of steady-state error and prevalence of noise [16,17].

As such, adaptive backstepping controller which specified identification of compatible Lyapunov function was simultaneously recommended towards operationalization of DC-DC buck/booster converter [18]. Showcased efficacy towards actualized application through exploitation of the adaptive rules is, nonetheless, counterbalanced by the approach's complicated layout and needed computation of redundant parameters [18,19]. Subsequently observed implementation of passivity-based control (PBC) towards coordinated handling of buck/boost converter within the work of [20] has alternatively limited its optimal applicability beyond superiorly modelled maneuvering of a DC-DC converter, besides its convoluted arithmetic requirements. Discussion centring previous exploration within this domain, therefore, corroborated unresolved hindrance in controller selection for DC-DC buck converter in light of the mechanisms' retained layout complexity, operator's requirement for extensive conceptual know-how, and reduced real-time precision on absence of modelled operational issues. The need to identify an utmost compatible control blueprint is hereby recognized towards the overcoming of mentioned setbacks.

Current proposition essentially pinpointed PID controller as the realistic control algorithm for DC-DC-buck converter. Note that the approach has remained vastly employed across an extensive span of industrial operations since its earlier inception, such application-wide approval was principally contributed by its minimized implementation requirement, simplified layout and functional proficiency [21]. Surfaced benefits then transpired multiple employments of PID-based approaches towards maneuvering of DC-DC buck converters, as per reported in [22–24]. With the technical realization where optimized parameters of proportional, derivative and integral gains would directly correlate exhibited efficacy of the current mechanism, necessitated requirement for a suitable optimization approach further propelled initialization of techniques such as Ziegler and Nichols (ZN) as of the year 1942 [25], alongside consecutive introduction of alternative techniques including Cohen Coon [26,27], Linear Quadratic Regulator (LQR) [28], pole placement [29], and gain-phase margin [30]. Having observed application of PID controller as optimized by the ZN method towards DC-DC buck converter within the work of [31], repeated experimentation through the process of trial-and-error by [32] contemporaneously uncovered subpar control precision under comparable implementation in term of extended proportional gains and overshoot with possible increase in oscillations from the method's relatively vigorous executing nature across progressive simulations. Renewed scholastic outlook, thus, switched the preference for metaheuristic tuning towards parametric optimization of PID controller on the account of iteration-based problem-solving for shortcomings within conventional tuning approaches through uncovering the optimized values at a global scale. Continuous expansion of the domain further exposed vast range of optimization techniques for the purpose of PID tuning to generate enhanced control precision from specified aspects of lowered settling interval, minimized overshoot and removed steady-state error.

Metaheuristic algorithms have shown excellent performance in current application such as in determining software requirement optimization [33,34], dynamic software rejuvenation optimal time prediction [35], path planning, solving the shortest path problem [36,37], data mining process [38], data processing [39] and biology and medicine [40–42]. Likewise, metaheuristic tuning of PID controller has demonstrated improved performance of the implemented DC-DC buck converter in multiple occasions. Such can be seen in the report by Emami regarding implementation of Particle Swarm Optimization (PSO) towards the aforementioned purpose, following successive rippling of a lowered output voltage from the DC-DC buck converter under maneuver of the optimized PID controller [43]. Comparison undertaken by Jalivand between algorithmic implementations of Bacterial Foraging Algorithm (BFA) and PSO towards parametric optimization of PID controller within structural layout which mirrored a DC-DC buck converter has uncovered superior operational outputs from the former technique [44]. Yusuf's support for benefits, efficacy and structural modesty of the Artificial Bee Colony (ABC) technique to tune the parameters of PID controller used in maneuvering DC-DC buck converter was verified on its overshadowing performance against application of the Genetic Algorithm (GA) from a shorter settling interval, diminished steady-state error and speedier reaction [45]. Undertaken simulation to investigate the capacity of PID controller as optimally tuned by the Cuckoo Search Algorithm (CSA) for minimized integral square error with respect to preferred outputs from a buck/boost converter, thus, succeeded an enhanced control performance against implementation of both GA and PSO techniques on lowered settling interval and elevated stability [46]. Pioneering of revised Flower Pollination Algorithm (FPA) by the hierarchical searching approaches by Wangtong for PID tuning of DC-DC buck converter defeated the optimization prowess of CSA on lower overshoot and heightened responsiveness to unstable load under the expense of overloaded computation across 1500 iterations [47]. Modernized approach to parametric optimization of PID for DC-DC buck converter saw the proposed engagement of Hybrid Whale Optimization Algorithm with Simulated Annealing (WOASAT) [48]. Having best-fitted resolution being determined by WOA prior attempting of Simulated Annealing (SA) towards finalized solution improvement and substitution, robustness of such hybridized technique would come with the price of complicated formula revision. Alternative tuning of PID controller towards enhanced performance of the DC-DC buck converter by mean of hybridized optimization technique saw an integration between Artificial Ecosystem-based Optimization (AEO) and the Nelder-Mead (NM) approach to overcome mediocre exploitation competency of AEO [49]. Workability of such decision was confirmed on outstanding results as yielded through implementation of the AEONM technique over its untouched AEO, PSO and DE

counterparts. Notable effectiveness of hybridized optimization techniques are conveniently observed from the results in [48] and [49] against standalone approaches for improved dynamism of PID-controlled DC-DC buck converter. Nevertheless, corresponding setback of immense computation from expansive determined coefficients and complicated formula revision need to be addressed through the search for other metaheuristic approaches pertaining lessen total coefficients.

Among the succeeding metaheuristic approaches then prevailed Sine Cosine Algorithm (SCA) by Mirjalili for PID's parametric identification which capitalized arithmetic functions of sine and cosine for search space exploration and exploitation between alternate routes to resolution of optimization issues [50]. Standardized performance appraisals substantially underlined the technique's superiority to adjacent metaheuristic approaches including Firefly Algorithm (FA), Bat Algorithm (BA), Flower Pollination Algorithm (FPA), Gravitational Search Algorithm (GSA), PSO, and GA [50]. Such track record is embellished by the technique's uncomplicated execution, capable search operation and reduced needs for parametric confirmation [51] in comparison with recent optimization algorithms such as Slime Mould Algorithm (SMA) [52], RIME algorithm (RIME) [53] and Harris Hawks Optimization (HHO) [54]. Presented versatility nonchalantly drove massive industrial applications, with the like of power generation through wind energy [55], economic power dispatch planning [56], networking [57], PID controller [58,59], image processing [60], and estimation of state-of-charge [61]. Noteworthy feasibility of SCA towards parametric optimization of the PID controller within DC-DC buck converter is supported through its previously discussed merits; yet, has not prevailed without any shortcoming. Primary concern highlights the degraded search ability of SCA from its disequilibrium in both undertaken exploration and exploitation. Recognized by the decreasing position-updated process within a conventional SCA through Eq. (3.4) which critically aids the one-way transition between the exploration and exploitation stages, exhibited linear transformation within such process is deemed less practical upon facing the need for nonlinear transformation within both stages in gaining an explicit global optima value. Equalized proportions between search domain exploring and exploiting, therefore, recognized the need for a compatible decreasing position-updated process. Secondary concern further uncovered the entrapment of search agent within the local optima which often correlates declined resolution variance, with lowered agent's capacity for positional withdrawal from said local optima domain. Conveyed and shared knowledge among agents regarding each's contemporary location amid the searching operation is proven detrimental under such circumstance from potential misguidance towards identical resolution domain with aggregate entrapment. Both identified obstacles should then be comprehensively assessed and tackled in fulfilling the development of an improved SCA technique.

Current pursuit for the above-mentioned objective of improving the conventional SCA approach radically driven initiation of two technical alterations. Development of the improved Sine Cosine Algorithm (ISCA) primarily offset disequilibrium between exploring and exploiting measures by readjustment of decreasing position-updated process as undertaken by the conventional algorithm. The nonlinear curve is hereby controlled by adoption of specified nonlinear decreasing operation under compatibly established coefficient as proposed within the work of [62] in seek of greater volatility as enabled by identification of suitable nonlinear formula towards proportioning of respective globalized exploring and localized exploiting. The setback of local optima entrapment secondarily pushed the installation of instrument which revises each search agent's average location as compulsory step in guiding its consequential withdrawal to assume further exploratory route pertaining assuring resolutions. This is achieved through revised location of individual agent within the operationalized instrument upon computed average across contemporary location of respective agent and the destination reference or best-fitted solution. The intention of appraising underlying efficacy of the updated ISCA approach was underlined through parametric identification of PID controller for effective maneuver of DC-DC buck converter by simulated virtue of statistical boxplots, non-parametric assessments, transient reaction, responsiveness to frequency, time-domain integral-error-performance indices, disturbance rejection and effectiveness against varying parameters. Besides the conventional SCA, generated outputs were contrasted alongside alternative algorithmic approaches of AEO, AEONM, PSO and DE [49]. Complete study would advance major contributions of

- I. Pioneering the implementation of both SCA and the currently introduced ISCA towards parametric optimization of the PID controller within a DC-DC buck converter.
- II. Instrument which revises each agent's average location was initialized through the updated ISCA approach. Such installation aided the withdrawal of agent trapped within the local optima domain to sustain its motions for unexplored route on possible solutions.
- III. Disequilibrium between the exploration and exploitation phases was addressed through reformed decreasing position-updated process of the conventional SCA by employment of nonlinear formula as reported in [62]. Collective endeavor pioneered an integrated outlook between both instrument which revises agents' average locations and the nonlinear formula in [62].
- IV. Performance evaluation of the introduced ISCA approach against preceding tuning algorithms from [49] for parametric optimization of PID controller used to maneuver the DC-DC buck converter enclosed numerous benchmarked assessments including response analysis, statistical performance analysis, time-domain integral-error-performance, frequency response analysis, disturbance rejection and parameter uncertainties analysis.

The current manuscript is structured as per: Key implementation and designing of the PID controller and the DC-DC buck converter are deliberated in Section 2. Section 3 shifted the attention for comprehensive interpretation of ISCA approach as currently developed towards parametric optimization of PID controller. Section 4 corroborates and contrasts the performance efficacy of PID controller as optimized by ISCA to its previous algorithm-based counterparts by standardized attempt of statistical boxplot analysis, non-parametric test analysis, transient response analysis, frequency response analysis, and time domain-based integral-error performance indices. The paper is conclusively summarized in Section 5.

1.1. Description of DC-DC buck converter

This section describes the conceptual layout overseeing implementation of PID as a controlling mechanism within the DC-DC buck converter. Arithmetic model for the DC-DC buck converter is primarily outlined. This is then followed by explanation regarding employment of the PID controller towards said application.

1.2. Modelling of the DC-DC buck converter

The DC-DC buck converter has been known for its classification as a switched-mode power supply (SMPS). Operating through intermittent switching of power output under immense frequency known as pulse wide modulation, the application essentially functions to lower higher level DC voltage. The circuit diagram presented in Fig. 1, thus, depicts a DC-DC buck converter which comprised the main source of DC voltage, voltage output, load resistance, filter inductor, filter capacitor, a switch and a diode as denoted by respective notation of V_g, V_o, R, L, C, S and D . Parametric specifications of the illustrated circuit for this study are then listed in alongside values for the appropriated reference voltage, $V_{ref} = 3V$, and switching frequency, $f_s = 40kHz$, as thoroughly adopted from the work of [49]. Assumption is further endorsed in accordance with [49,63] on the application's linear setting. Whereas arithmetic modelling for the DC-DC buck converter has been operationalized by mean of a switching signal-flow graph where modification would be attempted towards the application's circuitry arrangement upon contrasting switch conditions. Derivative process targeting specified model is simultaneously detailed within the work of [63]. Small-signal model of the application has also been exhibited in Fig. 1. Undertaken derivation by utilization of the Mason gain formula subsequently developed the arithmetic function for closed-loop transference in DC-DC buck converter as written by:

$$G_{vd}(s) = \frac{\Delta V_o(s)}{\Delta D(s)} = V_g \cdot \frac{\frac{1}{LC}}{s^2 + \frac{s}{RC} + \frac{1}{LC}} \tag{1}$$

1.3. PID controller for DC-DC buck converter system

A short review enclosing application of PID controller towards closed-loop manoeuvre of DC-DC buck converter for sustainable voltage output which conforms the appropriated magnitude is given within this section. A block diagram illustrating PID controller as employed within the DC-DC buck converter is primarily given in. Being a control method, which complied the feedback mechanism by identification of existing inaccuracy within application's output signal to its reference signal, parametric layout of the PID controller is hereby assumed by totalling of proportional, integral and derivative gains as independently represented by notations K_p, K_i , and K_d towards effective proceeding of control performance. Fundamentally, initialized computation of the error voltage, $\Delta V_e(s)$, through revealing apparent discrepancy between signals for the output voltage, $\Delta V_o(s)$, and appropriated voltage, $\Delta V_{ref}(s)$, would succeed well-fitted drafting of K_p, K_i , and K_d for the purpose of diminishing error voltage, $\Delta V_e(s)$. Generated output at the side of PID would then

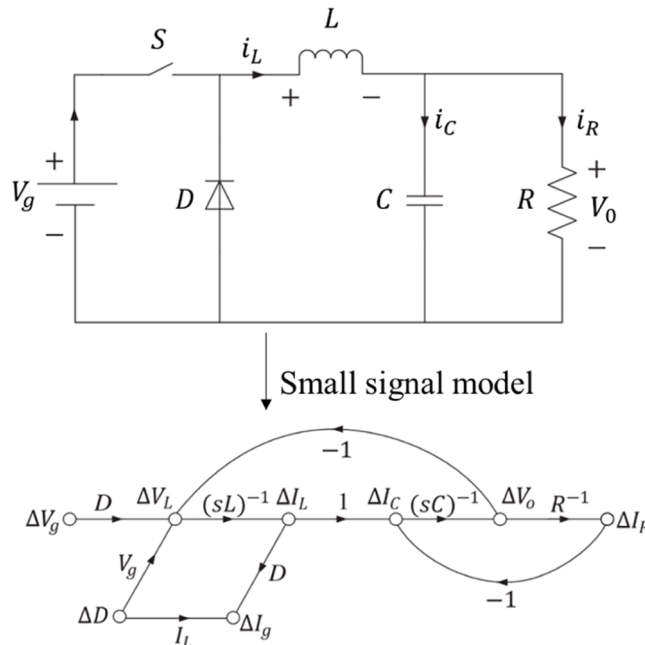


Fig. 1. DC-DC buck converter circuit and small signal model [49].

transpire actual manoeuvre of the DC-DC buck converter in achieving satisfactory transient reaction off output of $\Delta V_0(s)$ with substantial removal of steady-state error. Arithmetic equation governing transference process of the PID controller is hereby written as:

$$G_{PID}(s) = K_p + \frac{K_i}{s} + K_d s, \tag{2}$$

with the system's closed-loop transfer function in Fig. 2 being written as per the following:

$$T_{closed-loop}(s) = \frac{\Delta V_0(s)}{\Delta V_{ref}(s)} = \frac{G_{vd}(s) \times G_{PID}(s)}{1 + G_{vd}(s) \times G_{PID}(s)}, \tag{3}$$

where demonstrated output transitions and reference voltages are independently denoted by notations $\Delta V_0(s)$ and $\Delta V_{ref}(s)$.

Replacing Eqs. (1) and (2) towards Eq. (3) would consequently uncover the system's finalized closed-loop transfer function, with:

$$T_{closed-loop}(s) = \frac{216000 \times (K_d s^2 + K_p s + K_i)}{(0.0006s^3 + s^2 + 6000s + 216000) \times (K_d s^2 + K_p s + K_i)}, \tag{4}$$

where Table 1 is referenced for parameters of the DC-DC buck converter. The current study is hereby set to tackle aforementioned issue concerning control layout for rapid transient reaction, minimized overshoot and removal of steady-state error through acquisition of optimized parameters for PID controller towards enhanced operational outcomes of the DC-DC buck converter (Fig. 3).

2. Improved sine cosine algorithm (ISCA)

Explanation is given within the current section regarding implementation of the proposed ISCA algorithm towards parametric optimization of DC-DC buck converter with employment of the PID controller. Brief description centring the conventional SCA approach is primarily outlined, followed by a thorough discussion outlining alterations as undertaken within the ISCA approach. Subsequent explanation then delineates the tuning process by execution of ISCA algorithm towards parametric optimization of the DC-DC buck converter with PID controller.

2.1. Review of sine cosine algorithm (SCA)

This section focused inclusive consideration of the conventional SCA approach towards identification of its superior attributes and risen shortfalls which demand practical improvement. Being an algorithm founded by a multi-agent mechanism, the method as introduced by Mirjalili (2016) has based its inspiration from fundamental attributes of both sine and cosine functions. As such, primary exploration as initiated by the algorithm sets to obtain the global optima by developing an array of search agents as haphazardly scattered across the appointed search domain in seek of counteracting optimization issues comparable to that of the following:

$$\arg_{X_j(1), X_j(2), \dots} \min f_j(X_j(k)) \tag{5}$$

where both objective function and position vector for agent j are independently represented by respective notation of f_j and X_j . The current algorithm essentially resembles other optimization methods on differentiated iterative mechanisms between both exploration and exploitation phases. Undertaken process precipitously integrates arbitrary solutions across an array of solutions within the earlier exploration phase under immense impermanence of obtaining an assuring domain. However, a comparatively delayed process towards arbitrary solutions is adhered in the later exploitation phase with profoundly lesser randomized alterations against its preceding phase. Such tuning sequence would perpetually persist prior achievement of the maximum iterations. Locations pinpointing individual agent are further revised in accordance with the following:

$$X_{ij}(k+1) = X_{ij}(k) + r_1 \cdot \sin(r_2) \cdot |r_3 P_i - X_{ij}(k)|, \tag{6}$$

$$X_{ij}(k+1) = X_{ij}(k) + r_1 \cdot \cos(r_2) \cdot |r_3 P_i - X_{ij}(k)|, \tag{7}$$

where current location for agent j within the i th dimension of $i = 1, 2, \dots, d$ corresponding iteration k is denoted by notation $X_{ij}(k)$, with destination reference within the i th dimension being further denoted by notation P_i . Streamlined outlooks then denote the destination

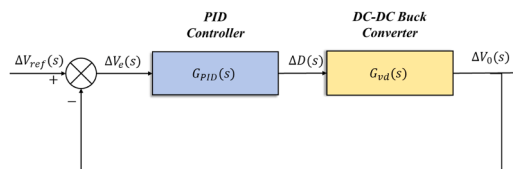


Fig. 2. DC-DC buck converter with PID controller.

Table 1
Parameters of the DC-DC buck converter [49].

Parameters	Symbols	Values
DC voltage	V_g	36 V
Load resistance	R	6 Ω
Filter inductor	L	1 mH
Filter capacitor	C	100 μ F
Steady-state duty cycle ratio	D	1/3

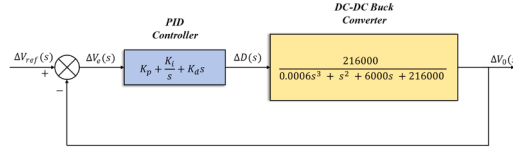


Fig. 3. Closed-loop transfer function of DC-DC buck converter with PID controller.

position vector which housed element P_i for acquisition of the finest solution using notation P , with the absolute value being simultaneously denoted by notation $\|$. Integration of both equations are then employed as per the following:

$$X_{ij}(k+1) = \begin{cases} X_{ij}(k) + r_1 \cdot \sin(r_2) \cdot |r_3 P_i - X_{ij}(k)|, & \text{if } r_4 < 0.5, \\ X_{ij}(k) + r_1 \cdot \cos(r_2) \cdot |r_3 P_i - X_{ij}(k)|, & \text{if } r_4 \geq 0.5, \end{cases} \quad (8)$$

where key randomized parameters of SCA are denoted by notation r_2 , r_3 , and r_4 as respectively segregated upon determined manoeuvre in approaching or distancing the destination reference through arbitrarily generated value spanning the scale of $[0, 2\pi]$, randomized magnitude of weight for the destination reference as arbitrarily selected across the numerical range of $[0, 2]$ towards confirming exiting gap to its contemporary location by arbitrarily accentuating or de-accentuating impact of the destination reference at respective notions of $r_3 > 1$ and $r_3 < 1$, and a value which falls within the range of $[0, 1]$ in conforming arbitrary transition between both sine and cosine functions. Equilibrium between the exploration and exploitation phases is pursued by all control algorithms towards uncovering assuring search domain with optimized convergence approaching global optima. Such operation would be endorsed by parametric component of r_1 within SCA by scheming sequential iterations of exploration and exploitation with accordance to equation as per the following:

$$r_1 = a - k \frac{a}{K_{max}}, \quad (9)$$

where both contemporary iteration and the highest number of iterations are denoted by notations k and K_{max} , respectively. Outlined statement, therefore, propelled SCA to undertake separate endeavours of exploring and exploiting the search domain upon respective condition of $r_1 > 1$ and $r_1 \leq 1$ as Fig. 4. Thorough characteristics of this algorithm is then detailed in the previous work of [50].

2.2. Improved sine cosine algorithm (ISCA)

Noteworthy benefits and applicability of the SCA approach towards resolution of various tuning issues have further accompanied apparent shortcomings of disequilibrium between undertaken exploration and exploitation processes, and potential trapping within the local optima. Such understanding then actuated a couple of propositions in the pursuit of algorithmic resolution towards enhanced control performance.

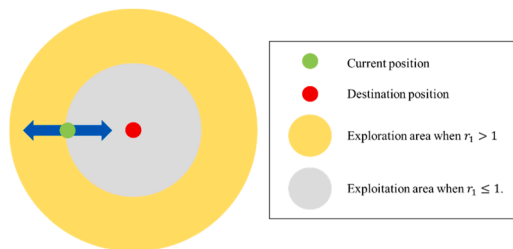


Fig. 4. The effect of parameter r_1 and exploration and exploitation phases [50].

2.3. Nonlinear equation of decreasing position-updated mechanism

Contrasting the position of r_1 within conventional SCA as the fundamental parametric component which progressively transforms revised operation across both exploring and exploiting endeavours, current proposition especially endorsed linear transition of said component with committed iterations proportionating the exploration and exploitation phases. Unfavourable aftereffect of an imbalanced exploration and exploitation distribution is hereby tackled following lowered precision of determined global optima through undue exploring, with lowered precision in undergone convergence through undue exploiting ensuing minimized potential of local optima avoidance. Nevertheless, such disequilibrium remained an elemental subset to numerous complicated engineering-related issues, whilst possibly restrained real-time feasibility of SCA under the recommended arrangement. Undertaken resolutions towards the aforementioned issues then pinpointed a need for revised equation of r_1 in elevating practitioner's resilience towards exploration and exploitation controls. Revised adaptation of r_1 for the current study with direct referencing to [62] is then defined as per the following:

$$\hat{r}_1 = a \times \sin\left(\left(1 - \frac{k}{K_{\max}}\right) \times \frac{\pi}{2}\right) + \beta, \quad (10)$$

where notation a is being determined as the value 2, with β being a positive value coefficient.

Convenient fabrication of exploration and exploitation operations by regulation of coefficient β is, therefore, achieved through revised computation of Eq. (10). Given plotted graphs in Fig. 5 which outlined both r_1 and computed \hat{r}_1 under dissimilar β values, greater number of iterations has been generated by the latter equation over the unimproved equation across all positive β values. Nonlinearity is hereby exhibited from gradual decline of \hat{r}_1 between respective values of $(a + \beta)$ and β prior the highest amount of iterations. Transformed proportion of iterations between both exploration and exploitation phases is then achieved through the current revision across initial optimization of coefficient β . An increased exploring endeavour from a higher β value for \hat{r}_1 , thus, allocates an extended interval for exploration beyond 65 % of maximized iterations at the expense of subsequent exploitation, vice versa. Given the optimistic outlook from [62] concerning feasibility of the revised \hat{r}_1 to an enhanced spectrum of real-time operations, optimized numerical preference to β would further ensure satisfactory equilibrium between both sequential phases in diminishing the primarily highlighted shortcomings.

2.4. Average position updating mechanism

Conventional SCA holds the negative potential of abrupt local optima entrapment by destination reference, P , without chances of withdrawal, whilst enraging possibility of hauling alternatively prevailed contemporary location of X_j towards the same domain. A chain reaction then ensues following local optima entrapment of former location, X_j , with simultaneous trapping of revised location, $X_j(k + 1)$, within said domain. Such outcomes have been the mechanistic implementation of sine and cosine functions under multiplication of absolute error to destination reference, P , and contemporary location, X_j , towards positional revision of individual agent with respect to contemporary location, X_j . Uncovered shortcoming is hereby resolved by structural implementation which revises the average location by mean of renewing subsequent location of each search agent through employed average enclosing both components of contemporary location, X_{ij} , and destination reference, P_i . Current alteration is then described as per the following:

$$A_{ij}(k) = \frac{X_{ij}(k) + P_i}{2}. \quad (11)$$

Taken directly off previous work of [52], averaging of iteration in its entirety further substantiated the absence of specific circumstance in which such mechanism can be implemented. Surfaced benefit is nonchalantly showcased on supports directed by destination point, P , towards assisting the escape of agent cornered within the local optima for subsequent proceeding of its updated exploratory route. Nevertheless, algorithmic enhancement to both undertaken exploration and exploitation is presented by operational virtue where search agent possesses the ability to withdraw from a trapped local optimum amid consecutive iterations in pursuit of its

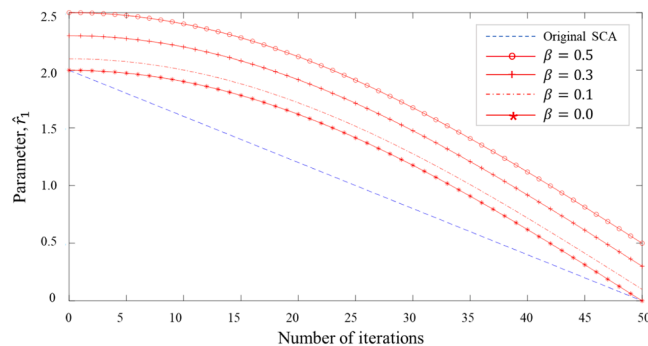


Fig. 5. The comparison of parameter \hat{r}_1 with different values of β .

final iteration. Contemporaneously revised implementation of SCA by the above-described alterations is given as:

$$X_{ij}(k+1) = \begin{cases} A_{ij}(k) + r_1 \cdot \sin(r_2) \cdot |r_3 P_i - X_{ij}(k)|, & \text{if } r_4 < 0.5 \\ A_{ij}(k) + r_1 \cdot \cos(r_2) \cdot |r_3 P_i - X_{ij}(k)|, & \text{if } r_4 \geq 0.5. \end{cases} \quad (12)$$

Systematic illustration demonstrating clarified depiction of undertaken operation for a revised average location is further given in Fig. 6. Presented deliberation focuses a pre-specified contour plot which placed the two-dimensional location of agent j , with agent cornered within the local optima being represented by a red-coloured triangle, X_j . As such, exclusive directory from contemporary location of X_j by employment of the conventional SCA would diminish the agent’s probability for positional withdrawal from said domain. Such restraint is swiftly resolved by inclusion of structural operation from the renewed equation towards revising its average location, as per exhibited through the green-coloured rectangle, A_j . Existence of A_j then compelled X_j ’s consequential probing of alternative exploratory route following aided withdrawal from its entrapment. Methodically sequenced through the procedure in Algorithm 1, improved SCA algorithm which goes by the name of Improved Sine Cosine Algorithm (ISCA), thus, integrates exceptional characteristics of an updated nonlinear equation and structural implementation for revised average location.

2.5. Application of the proposed ISCA for PID controller for DC-DC buck converter

Operationalization of the ISCA-PID controller as introduced within this study towards the DC-DC buck converter is explained within the current section. Employment of the ISCA algorithm typically endorsed the key purpose of parametric optimization for PID controller to achieve enhanced precision in operational outcomes. Currently attempted investigation further accounted comparable objective function to that of [49] which emphasized the specification of interval response known as the Figure of Demerit (FOD). Such objective function is further drawn as per the following:

$$FOD = (1 - e^{-\sigma}) \times (M_p + E_{ss}) + e^{-\sigma} \times (T_s + T_r), \quad (13)$$

where weighting coefficient as determined at 1×10^{-5} is denoted by notation σ , with the maximum overshoot, steady-state error, and rise and settling times being simultaneously represented by respective notations of M_p , E_{ss} , T_s , and T_r . Intended fulfilment of the operated system is then suggestively attainable by numerical modification to the weighting coefficient, σ , from the previously describe equation. Stated circumstance is hereby exemplified through specifying the weighting coefficient, σ , by adhering a designated range of $(1 \times 10^{-5}, 1 \times 10^{-4})$ in meeting system’s requirement for small M_p and reduced E_{ss} [49]. Likewise, value of σ as given in [49] has been reflectively adopted within the current study.

Comprehensive layout demonstrating employment and the flowchart of ISCA-PID to the DC-DC buck converter are subsequently exhibited in Figs. 7 and 8. Notably, the proposed ISCA algorithm would commence its operation through guidance from the objective function prior parametric optimization of the PID controller. Both objective function from Eq. (5) and the FOD function from Eq. (13) are hereby mapped by equalized function of $f_j = FOD$. Theoretical groundwork, thus, sufficed the optimization approach from ISCA on location of the agent, $X_j(k)$, following a diminished f_j . Sequential ranking of f_j as developed from individual $X_j(k)$ is, nonetheless, necessitated to uncover the finest f_j values, alongside their respective location, $X_j(k)$, or better goes by the destination reference of P . Eq. (12) is further employed towards a revised agent location, $X_j(k)$, with conforming updated parameters governing the PID controller within subsequent iteration. Described mechanism in its entirety shall continuously persist prior the highest number of iterations. Fragmentary steps encompassing the process is then summarized by:

3. Experimental results and discussion

Acquired findings centring robustness of DC-DC buck converter with implementation of the proposed ISCA-PID controller are deliberated within the current section. In accordance to the evaluative criteria as outlined below, comparison was made between performances of the proposed approach and preceding controllers of SCA-PID, AEONM-PID, AEO-PID, PSO-PID, and DE-PID [49].

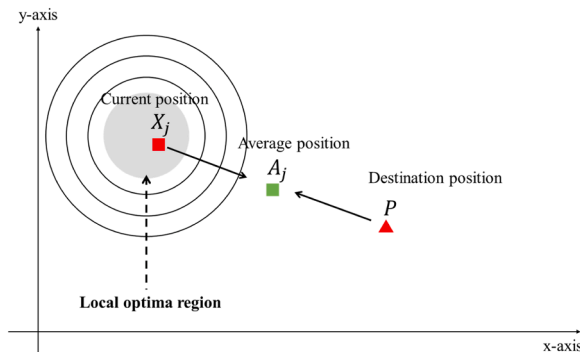


Fig. 6. Graphical representation of the average position updating mechanism.

Algorithm 1

Proposed ISCA algorithm.

1. Establish criteria for primary parameters: Upper and lower bounds (*ub* and *lb*), population size *N* (total search agents), maximized iterations (*K_{max}*), and coefficients *a* and *β*.
2. Arbitrarily load the location of individual search agent *X_j* (*j* = 1, 2, ..., *N*)
3. Assess objective function *f_j(X_j(*k*))*, whilst identify destination reference *P*.
4. **for** *k* = 1 : *K_{max}*
5. revise \hat{r}_1 using Eq. (10)
6. **for** *i* = 1 : *d*
7. **for** *j* = 1 : *N*
8. Separately generate arbitrary values for *r₂*, *r₃*, *r₄*
9. Acquire the revised location *X_{ij}*(*k*+1) by employment of Eq. (12) using the updated \hat{r}_1
10. **end for**
11. **end for**
12. Assess objective function *f_j(X_j(*k* + 1))*
13. **if** *f_j(X_j(*k* + 1))* < *f*(*P*)
14. *P* = *X_j*(*k* + 1)
15. **end if**
16. **end for**
17. Return *P* best solution acquired thus far

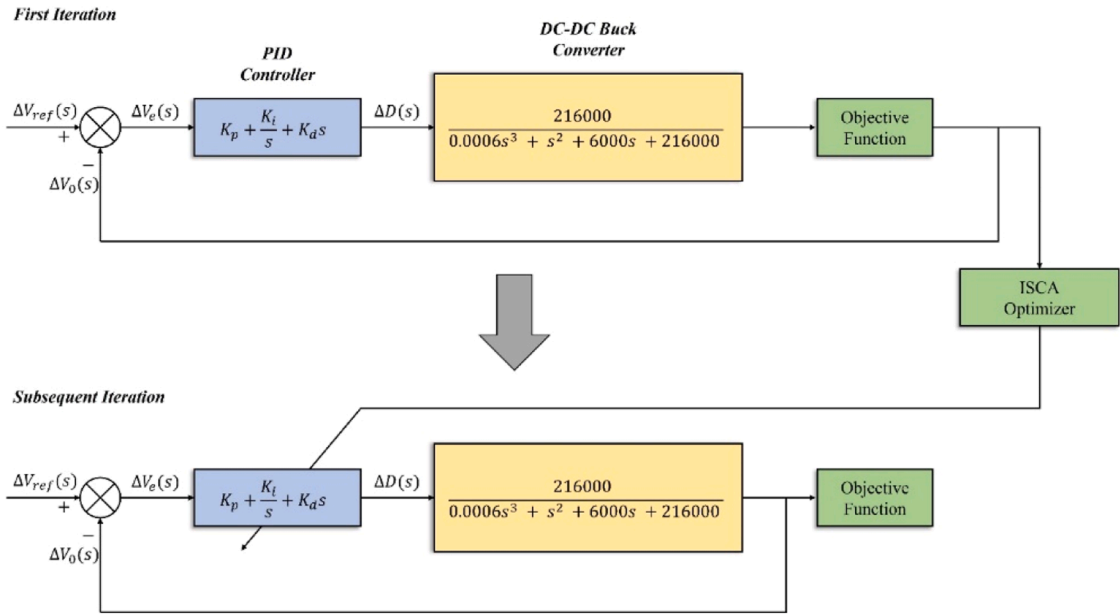


Fig. 7. DC-DC buck converter system with ISCA-PID controller.

1. Generated step response from the DC-DC buck converter was analysed from the aspects of peak value, overshoot, rise and settling times, and steady-state error.
2. Wilcoxon’s rank-sum test and box plot corresponding FOD function were employed to assess the non-parametric statistics through a total of 25 individual trials.
3. Indices corresponding time-domain integral-error-performance were compared on respective basis of integral of absolute error (IAE), integral of squared error (ISE), integral of time-weighted absolute error (ITAE), and integral of time-weighted squared error (ITSE). Each measurement of performance is mathematically composed as per the following:

$$ISE = \int_0^{t_s} (\Delta V_o(t) - \Delta V_{ref}(t))^2 dt, \tag{14}$$

$$IAE = \int_0^{t_s} |\Delta V_o(t) - \Delta V_{ref}(t)| dt, \tag{15}$$

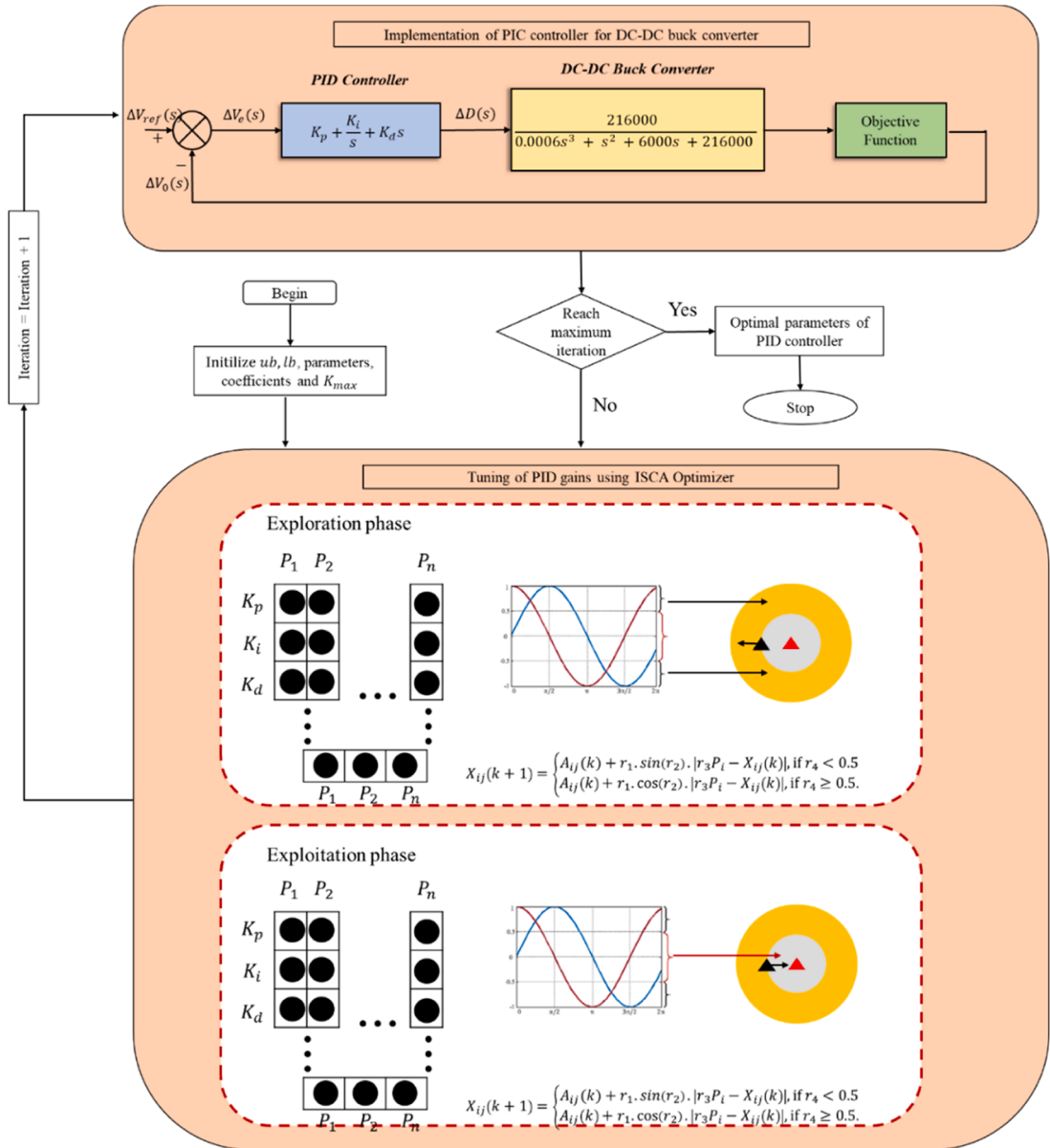


Fig. 8. The flowchart of the DC-DC buck converter system with a PID controller tuned by suggested ISCA.

$$\text{ITSE} = \int_0^{t_s} t \left((\Delta V_o(t) - \Delta V_{\text{ref}}(t))^2 \right) dt, \quad (16)$$

$$\text{ITAE} = \int_0^{t_s} t \left| \Delta V_o(t) - \Delta V_{\text{ref}}(t) \right| dt, \quad (17)$$

where the final simulation interval is denoted by t_s .

1. Bode plot as employed to analyse frequency reaction through appraised stability of the closed-loop system.
2. Efficacy of the DC-DC buck converter system as analysed against circumstance of parametric uncertainties.

Outlined components from [49] including total agents, maximum iterations, as well as the upper and lower bounds were identically appointed across the investigated algorithm-based PID approaches to ensure both validity and equality of undertaken performance appraisals. Such values were especially determined at $K_{\text{max}} = 50$ and $N = 24$ for both maximum number of iterations and total agents, with upper and lower bounds for parameters of the PID controllers being adopted as per Table 2. $\alpha = 2$ and $\beta = 0.03$ were further employed as coefficients to the proposed control algorithm. Such coefficients were then used to examine presented efficacy of ISCA in overcoming the impact of randomization under 25 individual trials. Predetermined standard of $\Delta V_{\text{ref}} = 3 \text{ V}$ under final simulation interval of $t_s = 10^{-5} \text{ s}$ was simultaneously accounted as reference voltage change of the current study.

3.1. Step response analysis

The current study specifically deliberates analysis conducted on time response as generated by DC-DC buck converter with implementation of the ISCA-PID controller. Importance of the analysis is founded on uncovering both speed and steady-state error to the system's output voltage response. Comparison was proceeded between efficacy of the proposed controller and alternative PID-based algorithms as recently introduced towards performance optimization of DC-DC buck converter. Plotted convergence curve corresponding the best FOD function of ISCA-PID from 25 individual trials has been exhibited in Fig. 9. Showcased outcomes adequately demonstrate competency of the proposed controller towards minimization of FOD function from Eq. (13) towards enhanced parametric optimization of the PID controller. Finest parametric values as determined for PID controller through employment of the proposed algorithm with respect to 25 individual trials against preceding algorithmic approaches are further outlined in Table 3.

Fig. 10 subsequently demonstrates recorded output voltage from the DC-DC buck converter in term of comparative transient and steady-state responses through implementation of SCA-PID and ISCA-PID, alongside preceding controllers of AEONM-PID, AEO-PID, PSO-PID, and DE-PID [49]. Arithmetic outputs for the components of peak value, percentage of overshoot, rise and settling times, and steady-state error are then comparatively tabulated in Table 4. While collective results fundamentally proposed steady responses at the absence of overshoot and steady-state error from each examined algorithm-based PID approaches, ISCA-PID controller as per currently introduced has further superseded performance of other alternatives on the shortest rise and settling times. Enhanced precision against preceding approaches further corroborated ISCA-PID as the better controller towards excellent operational response.

3.2. Statistical performance analysis

The current subsection set to compare athenatic results centring statistical outcomes from FOD function of the DC-DC buck converter through implementation of ISCA-PID and its preceding algorithm-based PID approaches. Acquired values for the best, mean and standard deviation of FOD function across 25 individual trials through implementation of the currently examined controllers are further itemized in Table 5. Presented findings hereby exhibit the lowest best, mean and standard deviation values from the proposed ISCA-PID controller over its predecessors. As such, evaluated outcomes support the efficacy of ISCA-PID across majority of the attempted trials towards pinpointing of optimal parametric values for the DC-DC buck converter.

Boxplots specifying FOD function of independent algorithm as examined within the current study across 25 independent trials are subsequently outlined in Fig. 11. Herewith, both the lowest and highest values retained are respectively represented by the discontinued, black-colored lines stretched from lower and upper sides of the box which go by the name of whiskers, with the median for

Table 2
Upper bound and lower bound of PID controller [49].

Parameter	Lower bound, (<i>lb</i>)	Upper bound, (<i>ub</i>)
K_p	1	50
K_i	0.01	10
K_d	0.001	0.01

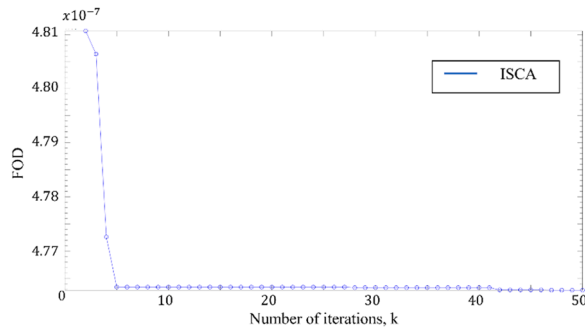


Fig. 9. Convergence curve of the best objective function from 25 trials.

Table 3
Optimal PID controller parameters.

Algorithm	K_p	K_i	K_d
ISCA-PID (proposed)	17.0320	7.09308	0.01000
SCA-PID	17.0304	0.0100	0.01000
AEONM-PID [49]	16.8278	1.1742	0.00992
AEO-PID [49]	33.1153	7.9506	0.00943
PSO-PID [49]	37.1502	3.7225	0.00821
DE-PID [49]	27.6235	1.3043	0.00873

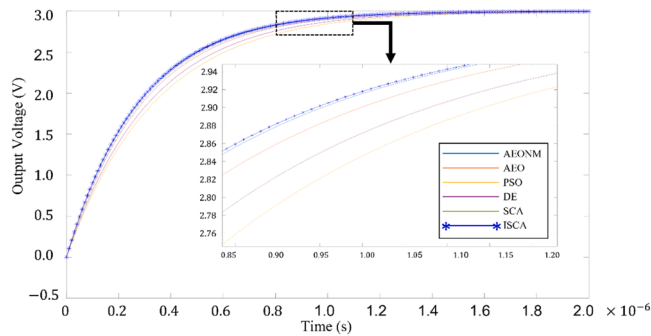


Fig. 10. Output voltage responses comparisons of the DC-DC buck converter system.

Table 4
Output voltage response performance for different algorithm-based PID controllers.

Algorithm	Peak value (V)	Overshoot (%)	Rise time (s)	Settling time (s)	Steady-state error (V)
ISCA-PID (proposed)	3.0000	0	6.10317754E-07	1.08660835E-06	0
SCA-PID	3.0000	0	6.10317836E-07	1.08660891E-06	0
AEONM-PID [49]	3.0000	0	6.1519E-07	1.0954 E-06	0
AEO-PID [49]	3.0000	0	6.4613E-07	1.1454 E-06	0
PSO-PID [49]	3.0000	0	7.4122E-07	1.3093 E-06	0
DE-PID [49]	3.0013	0.0438	6.9808E-07	1.2381 E-06	0

Table 5
The statistical performance value of the FOD function of the proposed ISCA-PID controller compared to other algorithm-based PID controllers.

Algorithm	Best	Mean	Standard deviation
ISCA-PID (proposed)	4.7627E-07	4.7627E-07	6.8515E-12
SCA-PID	4.7627E-07	4.7628E-07	3.8511E-11
AEONM-PID [49]	4.8016E-07	4.9563E-07	1.4493E-08
AEO-PID [49]	4.9920E-07	5.1693E-07	1.6234E-08
PSO-PID [49]	5.6805E-07	5.8939E-07	1.5587E-08
DE-PID [49]	5.6191E-07	5.8340E-07	1.9324E-08

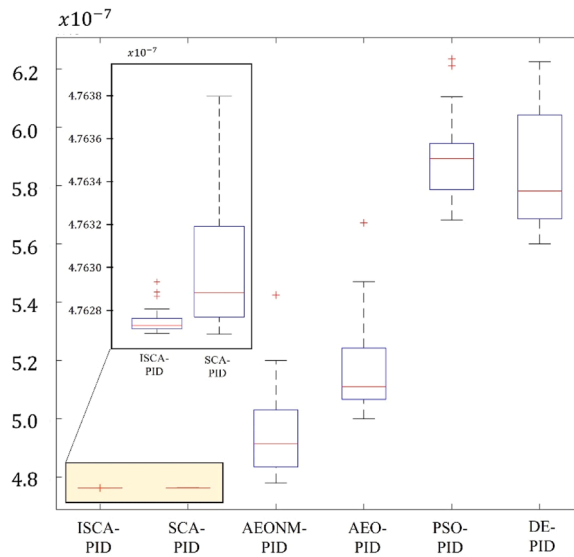


Fig. 11. Box plot of the FOD function produced by different algorithm-based PID controllers.

each algorithm being further represented by red-colored line crossing the internal section of each box. Identified outliers beyond the lowest and highest retained values are then independently represented by an intersected symbol within the collective diagram. Relatively shorter interquartile ranges for the boxplots as developed by both SCA-PID and ISCA-PID, therefore, verified the controllers’ performance superiority against other preceding alternatives. Magnified evaluations on the prevailed controllers further demonstrated the distributive excellence of ISCA-PID over its conventional version. Operational outcomes with comparatively higher consistency from ISCA-PID ultimately backed the current stipulation on an enhanced maneuver and precision across majority of the attempted trials against other examined control alternatives.

Additional outlook then appraised the acquired results from Wilcoxon’s rank-sum test corresponding FOD function across the proposed ISCA-PID method and other preceding controllers as examined within this study with adhering a significance level of 5 %. Unachieved by other algorithm-based control approaches, numerical findings as tabulated in Table 6 essentially exhibit a p-value smaller than 0.05 through implementation of the ISCA-PID controller. Such discovery, thus, recognized greater significance for FOD function from ISCA-PID over the preceding approaches of SCA-PID, AEONM-PID, AEO-PID, PSO-PID and DE-PID.

3.3. Comparison of time-domain integral-error-performance

The current subsection compared the proposed ISCA-PID controller to other algorithm-based PID approaches as underlined within this study on the ground of operational error by common virtue of integral square error (ISE), integral absolute error (IAE), integral of the time squared error (ITSE), and integral of the absolute error weighted over time (ITAE). Evaluation towards each approach was attempted by computation of operational indicators as specified within Eq. (10) to Eq. (12) following optimized parametric values of the controllers as stated in Table 3 under the designated simulation interval of $t_s = 10^{-5}$ s. Outlined findings of each algorithm-based PID controller in Fig. 12 then shows smaller outputs for both ISCA-PID and its unimproved method against other examined control alternatives with respect to collective error-related domains of ISE, IAE, ITSE and ITAE. Comparative evaluation through tabulated information in Table 7 further distinguished ISCA-PID as the best approach across examined algorithmic methods in light of its lowest value of outputs.

3.4. Frequency response analysis

The current subsection compared Bode plots as developed from the DC-DC buck converter by implementation of SCA-PID and ISCA-PID against earlier PID-based approaches being examined within this study in comparatively assessing the operational stability as exerted by a closed-loop structure by employment of the proposed approach to that of its algorithmic predecessors. Nevertheless, Fig. 13 specifically illustrates both magnitude and phase plots corresponding Bode diagram for ISCA-PID, with comprehensive

Table 6
Wilcoxon’s rank-sum test of the FOD function for ISCA-PID and other algorithm-based PID controllers.

Algorithm	ISCA-PID vs SCA-PID	AEONM-PID [49]	AEO-PID [49]	PSO-PID [49]	DE-PID [49]
p-value	8.5725E-06	1.5821E-14	1.5821E-14	1.5821E-14	1.4144E-09

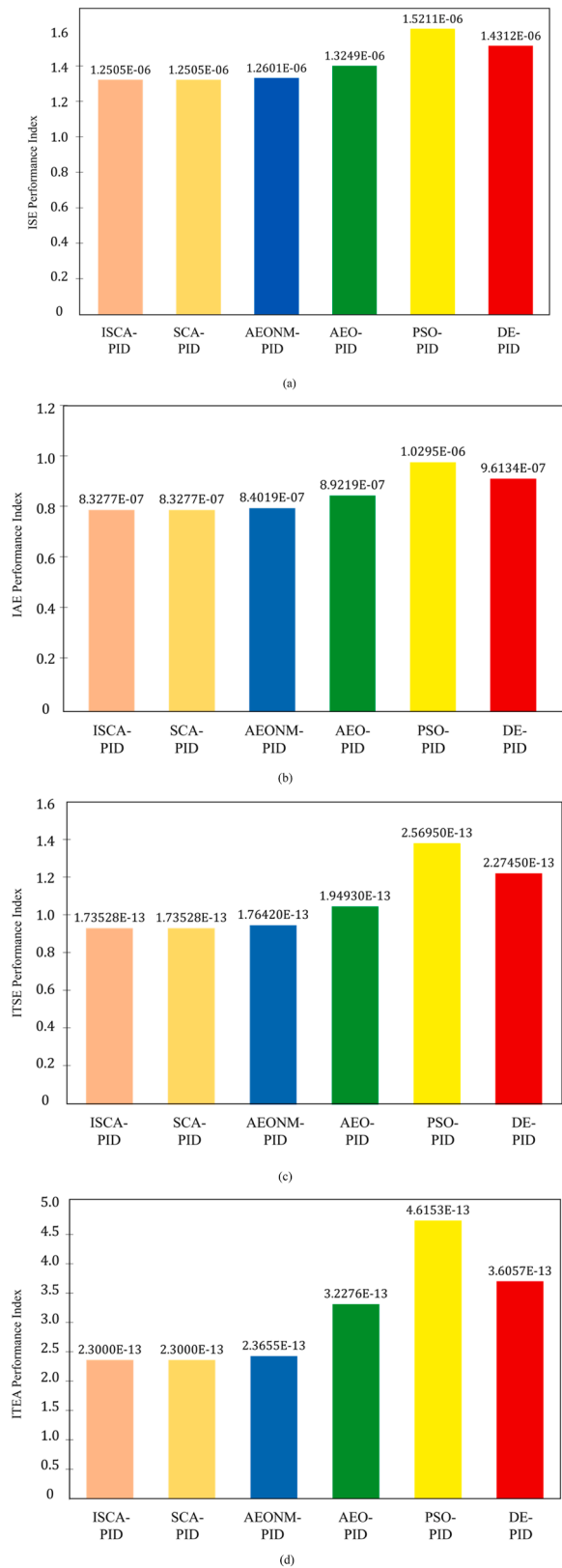


Fig. 12. Comparison of the (a) ISE performance index, (b) IAE performance index, (c) ITSE performance index and (d) ITAE performance index produced by different algorithm-based PID controllers [49].

Table 7

Comparison of difference errors, ISE, IAE, ITSE, and ITAE produced by different algorithm-based PID controllers.

	ISCA-PID	SCA-PID	AEONM-PID [49]	AEO-PID [49]	PSO-PID [49]	DE-PID [49]
ISE	1.25052756E-06	1.25052762E-06	1.26010000E-06	1.32490000E-06	1.52110000E-06	1.43120000E-06
IAE	8.32766456E-07	8.32766649E-07	8.40190000E-07	8.92190000E-07	1.02950000E-06	9.61340000E-07
ITSE	1.73528446E-13	1.73528476E-13	1.76420000E-13	1.94930000E-13	2.56950000E-13	2.27450000E-13
ITAE	2.29998998E-13	2.29999235E-13	2.36550000E-13	3.22757000E-13	4.61530000E-13	3.60570000E-13

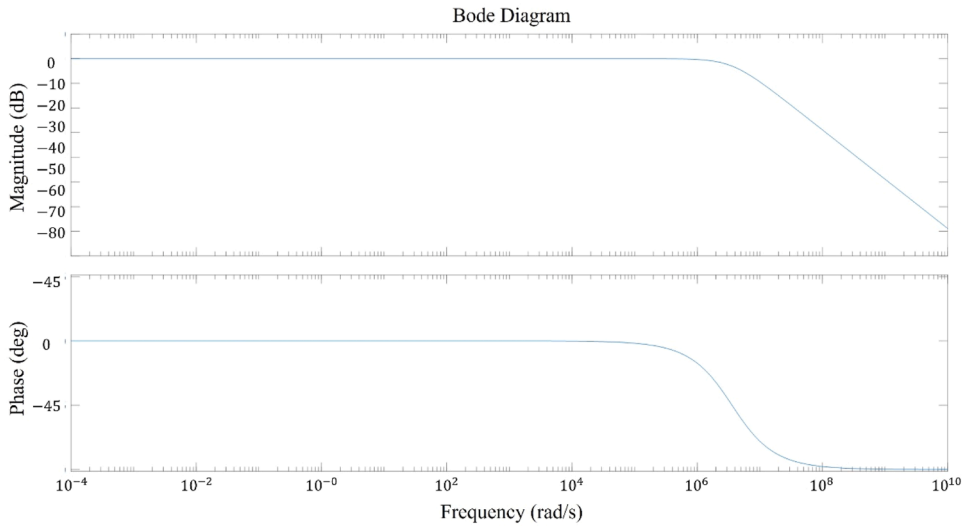


Fig. 13. Bode plot of the proposed ISCA-SPID controller.

performance outputs enclosing gain and phase margins, as well as bandwidth from each examined PID-based approaches being further tabulated in Table 8. Having observed comparable results on the component of gain margin across all examined algorithmic approaches, ISCA-PID has markedly outshined its predecessors on counts of a greater bandwidth. Such revelation essentially endorsed the superior response efficacy of DC-DC buck converter towards incoming frequency by implementation of the proposed ISCA-PID controller.

3.5. Disturbance rejection analysis

Crucial trait accompanying an effectively manoeuvred system further suggested the ability to counteract unforeseen disturbances. Robustness of the DC-DC buck converter with separate implementation of ISCA-PID and its preceding PID-based approaches was, therefore, appraised within the current subsection under the influence of external disturbance. Achieved by replicating the formerly simulated appraisal with presence of signalled disturbance, equivalent block diagram centring the DC-DC buck converter facing the currently investigated circumstance is further demonstrated in Fig. 14, with amplitude of signalled disturbance as exhibited in Fig. 15 being contemporaneously determined at a value of 0.5. Operated simulation then applied said disturbance at $\Delta V_{ref} = 0$ V to imitate transformed load within an actual occurrence of power electronics, with acquired findings for the proposed controller and its algorithmic predecessors being collectively tabulated in Fig. 16. Comparative evaluation hereby substantiated a shorter settling interval by both ISCA-PID and SCA-PID at identical outcome of 1.0865E-06 s over other examined control alternatives of AEONM-PID, AEO-PID, DE-PID and PSO-PID at respective outcome of 1.052E-06 s, 1.1525E-06 s, 1.2449E-06 s and 1.3241E-06 s. Generated findings, thus, verified the overshadowing competency of ISCA-PID and SCA-PID against their PID-based counterparts within operational domain of disturbance rejection.

Table 8

Stability measure comparison of different algorithm-based PID controllers.

	Gain margin (dB)	Phase margin (deg)	Bandwidth (Hz)
ISCA-PID	infinite	180	3.5916E+06
SCA-PID	infinite	180	3.5915E+06
AEONM-PID [49]	infinite	180	3.5628E+06
AEO-PID [49]	infinite	178.1149	3.3886E+06
PSO-PID [49]	Infinite	177.4863	2.9515E+06
DE-PID [49]	Infinite	178.2405	3.1369E+06

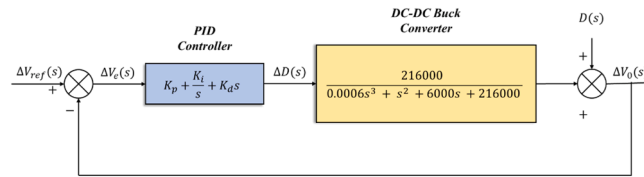


Fig. 14. DC-DC buck converter with the existence of disturbance $D(s)$.

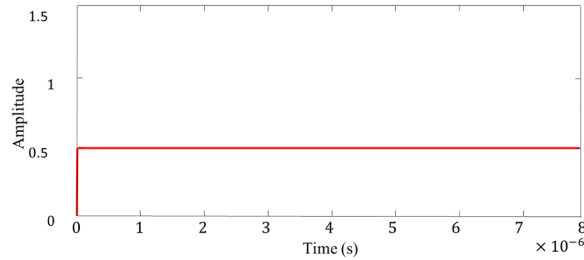


Fig. 15. Disturbance signal, $D(s)$.

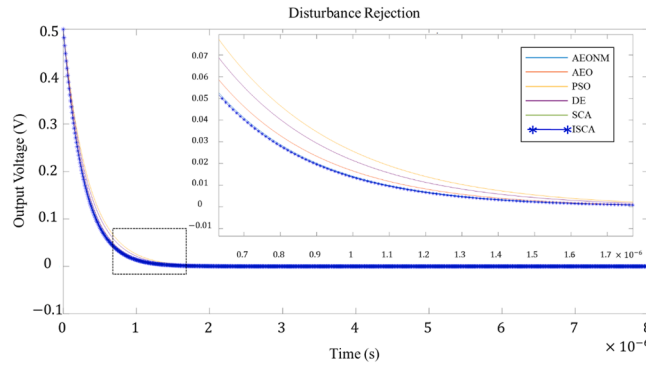


Fig. 16. System response with disturbance.

3.6. Parameter uncertainties analysis

Experimentation centring parametric uncertainties was hereby operationalized in assessing the competency of ISCA-PID controller towards managing transformative parametric dissimilarities of the examined DC-DC buck converter. A parameter uncertainties analysis was, therefore, conducted by specifying respective range of -20% and $+20\%$, and -10% and $+10\%$ as the parameters for L and C to observe the step response of DC-DC buck converter through separate implementation of each investigated algorithm-based PID approach from its comprehensive aspects of peak value, overshoot, rise and settling times, and steady-state error. Tabulated results in Table 9 have essentially exhibited an unchanged peak value, overshoot and steady-state error through application of ISCA-PID under the smallest rise and settling times upon facing altered parametric values of L and C . Such outcomes, thus, sufficed a uniformly satisfactory response from the proposed method against encountered irregularities across parameters of the DC-DC buck converter.

4. Conclusion

The current study set to optimize parametric values of PID controller as employed within the DC-DC buck converter through implementation of an Improved Sine Cosine Algorithm (ISCA). Optimization of the employed controller was especially undertaken through two separate alterations to the conventional Sine Cosine Algorithm (SCA). Enhanced efficacy was successively achieved from the ISCA approach by virtue of the smallest rise ($6.10317754E-07$) and settling times ($1.08660835E-06$) under an excellent FOD value. Such outcomes are further substantiated by improved statistical results on both counts of Wilcoxon’s signed-rank test and box plots analysis. Diminished values for the components of ISE ($1.25052756E-6$), IAE ($8.32766456E-7$), ITSE ($1.73528446E-13$) and ITAE ($2.29998998E-13$) upon facing an array of dissimilar operational circumstances against preceding algorithm-based PID controllers then conformed the proposed approach as a comparatively superior optimizing alternative. Likewise, satisfactory results have been recorded for responses exhibited by the method towards frequency from the examined system within a Bode plot simulation.

Table 9
Robustness analysis results of the proposed ISCA-PID controller.

Parameter	Rate of change	Algorithm	Peak value (V)	Overshoot (%)	Rise time (s)	Settling time (s)	Steady-state error (V)		
L	-20%	ISCA-PID	3.0000	0	4.8768E-07	8.6565E-07	0		
		SCA-PID	3.0000	0	4.8769E-07	8.6566E-07	0		
		AEONM-PID [49]	3.0000	0	4.9215E-07	8.7631E-07	0		
		AEO-PID [49]	3.0012	0.04	5.1707E-07	9.1740E-07	0		
		PSO-PID [49]	3.0000	0	5.9331E-07	1.0497E-06	0		
		DE-PID [49]	3.0010	0.0346	5.5862E-07	9.9157E-07	0		
	+20%	ISCA-PID	3.0000	0	7.3115E-07	1.2957E-06	0		
		SCA-PID	3.0000	0	7.3116E-07	1.2958E-06	0		
		AEONM-PID [49]	3.0000	0	7.3822E-07	1.3144E-06	0		
		AEO-PID [49]	3.0000	0	7.7511E-07	1.3727E-06	0		
		PSO-PID [49]	3.0003	0.0096	8.8896E-07	1.5679E-06	0		
		DE-PID [49]	3.0000	0	8.3746E-07	1.4842E-06	0		
		C	-10%	ISCA-PID	3.0000	0	5.4860E-07	9.7332E-07	0
				SCA-PID	3.0000	0	5.4861E-07	9.7333E-07	0
AEONM-PID [49]	3.0000			0	5.5375E-07	9.8636E-07	0		
AEO-PID [49]	3.0012			0.0404	5.8170E-07	1.0320E-06	0		
PSO-PID [49]	3.0000			0	6.6740E-07	1.1804E-06	0		
DE-PID [49]	3.0010			0.0339	6.2846E-07	1.1156E-06	0		
+10%	ISCA-PID		3.0000	0	6.7032E-07	1.1883E-06	0		
	SCA-PID		3.0000	0	6.7033E-07	1.1884E-06	0		
	AEONM-PID [49]		3.0001	0.0022	6.7661E-07	1.2043E-06	0		
	AEO-PID [49]		3.0000	0	7.1053E-07	1.2584E-06	0		
	PSO-PID [49]		3.0002	0.0058	8.1497E-07	1.4379E-06	0		
	DE-PID [49]		3.0000	0	7.6766E-07	1.3604E-06	0		

Conducted analysis on both disturbance rejection and parameter uncertainties subsequently demonstrated progressive refitting of the employed ISCA-PID controller towards disturbance signals and detected transitions across parameters of the SC-SC buck converter. Collective findings on greater precision and stability essentially braced admirable compatibility of ISCA-PID towards numerous controlling functions over other existing algorithm-based PID approaches. Promising effects as posited by the currently endorsed alterations on conventional SCA further showcased compelling applicability in resolving comparable setbacks of other optimization approaches. Nevertheless, validated proficiency of the proposed ISCA method is, nonetheless, applicable towards overcoming wide range of real-time issues spanning various engineering-related operations such as DC motor speed control, automatic voltage regulator, power system stabilizer and so on. Therefore, for future research direction, the performance of the proposed ISCA-PID may be further improved by upgrading the flexibility of flexibility to control the exploration and exploitation phases. Secondly, the ISCA can be hybridized with other algorithms to improve its performance. Hence, a more general class of DC-DC Buck controller can be obtained while the control accuracy is improved.

Declaration of Competing Interest

The authors declare that they have no known competing financial interests or personal relationships that could have appeared to influence the work reported in this paper.

Data availability

No data was used for the research described in the article.

Acknowledgment

Utmost Gratitude is directed to Universiti Malaysia Pahang Al-Sultan Abdullah for the financial assistance offered through the internal UMP Research Grant Scheme RDU223011.

References

- [1] Hasanpour S, Siwakoti YP, Blaabjerg F. A new high efficiency high step-up DC/DC converter for renewable energy applications. *IEEE Trans Ind Electron* 2023;70(2):1489–500. <https://doi.org/10.1109/TIE.2022.3161798>.
- [2] Jyotheeswara Reddy K, Natarajan S. Energy sources and multi-input DC-DC converters used in hybrid electric vehicle applications – A review. *Int J Hydrogen Energy* 2018;43(36):17387–408. <https://doi.org/10.1016/j.ijhydene.2018.07.076>.
- [3] Nan C, Ayyanar R, Xi Y. A 2.2-MHz active-clamp buck converter for automotive applications. *IEEE Trans Power Electron* 2018;33(1):460–72. <https://doi.org/10.1109/TPEL.2017.2672522>.
- [4] Dam S, Mandal P. A hybrid, fully-integrated, dual-output DC-DC converter for portable electronics. *IEEE Trans Power Electron* 2021;36(4):4360–70. <https://doi.org/10.1109/TPEL.2020.3019273>.

- [5] Wu Z, Shen S, Lian X, Su X, Chen E. A dummy-based user privacy protection approach for text information retrieval. *Knowl Based Syst* 2020;195:105679. <https://doi.org/10.1016/J.KNOSYS.2020.105679>.
- [6] Wu Z, Xuan S, Xie J, Lin C, Lu C. How to ensure the confidentiality of electronic medical records on the cloud: a technical perspective. *Comput Biol Med* 2022;147:105726. <https://doi.org/10.1016/J.COMPBIOMED.2022.105726>.
- [7] Wu Z, Shen S, Li H, Zhou H, Lu C. A basic framework for privacy protection in personalized information retrieval: an effective framework for user privacy protection, vol. 33, no. 6, pp. 1–26, 2021.
- [8] Wu Z, Li G, Shen S, Lian X, Chen E, Xu G. Constructing dummy query sequences to protect location privacy and query privacy in location-based services. *World Wide Web* 2021;24(1):25–49. <https://doi.org/10.1007/s11280-020-00830-x>.
- [9] Wu Z, Shen S, Zhou H, Li H, Lu C, Zou D. An effective approach for the protection of user commodity viewing privacy in e-commerce website. *Knowl Based Syst* 2021;220:106952. <https://doi.org/10.1016/j.knosys.2021.106952>.
- [10] Wu Z, Xie J, Shen S, Lin C, Xu G, Chen E. A confusion method for the protection of user topic privacy in Chinese keyword-based book retrieval. *ACM Trans Asian Low Resour Lang Inf Process* 2023;22(5):1–19.
- [11] Ghamari SM, Mollaei H, Khavari F. Robust self-tuning regressive adaptive controller design for a DC–DC BUCK converter. *Measurement* 2021;174:109071. <https://doi.org/10.1016/j.measurement.2021.109071>. 174.
- [12] Hart DW. *Power Electronics*. New York: McGraw-Hill Companies, Inc; 2010.
- [13] Sheehan R, Diana L. Switch-mode power converter compensation made easy, Texas Instruments Power Supply Design Seminar, pp. 1–38, 2016.
- [14] Ramya HS, Sangeetha K, Shashirekha M, Varalakshmi K. Design of compensator for DC-DC buck converter. *Int J Innov Res Technol Sci IJIRTS* 2023;3:35–40. VolNo.
- [15] Salimi M, Soltani J, Zakipour A, Hajbani V. Sliding mode control of the DC-DC flyback converter with zero steady-state error. In: Proceedings of the 4th annual international power electronics, drive systems and technologies conference; 2013. p. 158–63. <https://doi.org/10.1109/PEDSTC.2013.6506695>.
- [16] Chen Z. PI and sliding mode control of a cuk converter. *IEEE Trans Power Electron* 2012;27(8):3695–703. <https://doi.org/10.1109/TPEL.2012.2183891>.
- [17] Padhyay SB, Panda Prof GK, Saha Prof PK, Das Prof S. Advance control techniques for DC/DC buck converter with improved performance. *Int J Adv Res Electr Electron Instrum Eng* 2015;04(01):201–8. <https://doi.org/10.15662/ijareeie.2015.0401029>.
- [18] Salimi M, Soltani J, Zakipour A. Adaptive nonlinear control of DC-DC buck/boost converters with parasitic elements consideration. In: Proceedings of the international conference on control, instrumentation and automation (ICCIA); 2011. p. 304–9. <https://doi.org/10.1109/ICCIAutom.2011.6356674>.
- [19] Coban R. Adaptive backstepping sliding mode control with tuning functions for nonlinear uncertain systems. *Int J Syst Sci* 2019;50(8):1517–29. <https://doi.org/10.1080/00207721.2019.1615571>.
- [20] Salimi M, Eghlim AL. Passivity-based control of the DC-DC buck converters in high-power applicationse. In: Proceedings of the IEEE region 10 annual international conference, proceedings/TENCON; 2015. <https://doi.org/10.1109/TENCON.2014.7022387>. 2015-Janua.
- [21] Suid MH, Ahmad MA. Optimal tuning of sigmoid PID controller using nonlinear sine cosine algorithm for the automatic voltage regulator system. *ISA Trans* 2022;128:265–86. <https://doi.org/10.1016/j.isatra.2021.11.037>.
- [22] Mingzhi H, Jianping X. Nonlinear PID in digital controlled buck converters. In: Proceedings of the conference proceedings - IEEE applied power electronics conference and exposition - APEC; 2007. p. 1461–5. <https://doi.org/10.1109/APEX.2007.357709>.
- [23] Zhou C, Zhang Q, Ezechias DD, Gao Y, Deng H, Qu S. A general digital PID controller based on PWM for buck converter. In: Proceedings of the world congress on intelligent control and automation (WCICA); 2014. p. 4596–9. <https://doi.org/10.1109/WCICA.2014.7053488>.
- [24] Guo L, Hung JY, Nelms RM. PID controller modifications to improve steady-state performance of digital controllers for buck and boost converters. In: Proceedings of the APEC. Seventeenth annual IEEE applied power electronics conference and exposition (Cat. No.02CH37335). IEEE; 2002. p. 381–8. <https://doi.org/10.1109/APEC.2002.989274>.
- [25] Ziegler JG, Nichols NB. Optimum settings for automatic controllers. *Trans ASME* 1942;(64):759–68.
- [26] Isdaryani F, Feriyonika F, Ferdiansyah R. Comparison of Ziegler-Nichols and Cohen Coon tuning method for magnetic levitation control system. *J Phys Conf Ser* 2020;1450(1):012033. <https://doi.org/10.1088/1742-6596/1450/1/012033>.
- [27] Utami AR, Yuniar RJ, Giyantara A, Saputra AD. Cohen-Coon PID tuning method for self-balancing robot. In: Proceedings of the international symposium on electronics and smart devices (ISESD); 2022. p. 1–5. <https://doi.org/10.1109/ISESD56103.2022.9980830>.
- [28] Srivastava S, Kumar Y, Misra A, Thakur SK, Pandit VS. Optimum design of buck converter controller using LQR approach. In: Proceedings of the international conference on advanced computing technologies (ICACT2013), IEEE computer society; 2013. p. 1–6. <https://doi.org/10.1109/ICACT.2013.6710514>.
- [29] Andries VD, Goras L, David E, Buzo A, Pelz G. On the pole-placement technique for the design of a DC-DC buck converter discrete PID control. In: Proceedings of the 23rd international symposium on design and diagnostics of electronic circuits & systems (DDECS), Apr; 2020. <https://doi.org/10.1109/DDECS50862.2020.9095562>.
- [30] Shehada A, Yan Y, Beig AR, Boiko I. Auto-tuning of PID controller with gain margin specification for digital voltage-mode buck converter. *IFAC PapersOnLine* 2020;53(2):13390–5. <https://doi.org/10.1016/j.ifacol.2020.12.176>.
- [31] Lindiya A, Palani S, Iyyappan M. Performance comparison of various controllers for DC-DC synchronous buck converter. *Procedia Eng* 2012;38:2679–93. <https://doi.org/10.1016/j.proeng.2012.06.315>.
- [32] Razak Ramesh NHA, Ghazali MR, Ahmad MA. Sigmoid pid based adaptive safe experimentation dynamics algorithm of portable duodopa pump for parkinson's disease patients. *Bull Electr Eng Inform* 2021;10(2):632–9. <https://doi.org/10.11591/eei.v10i2.2542>.
- [33] Alrezaamiri H, Ebrahimnejad A, Motameni H. Software requirement optimization using a fuzzy artificial chemical reaction optimization algorithm. *Soft Comput* 2019;23(20):9979–94. <https://doi.org/10.1007/S00500-018-3553-7/METRICS>.
- [34] Alrezaamiri H, Ebrahimnejad A, Motameni H. Parallel multi-objective artificial bee colony algorithm for software requirement optimization. *Requir Eng* 2020;25(3):363–80. <https://doi.org/10.1007/S00766-020-00328-Y/METRICS>.
- [35] Kalantari KR, Ebrahimnejad A, Motameni H. Efficient improved ant colony optimisation algorithm for dynamic software rejuvenation in web services. *IET Softw* 2020;14(4):369–76. <https://doi.org/10.1049/IET-SEN.2019.0018>.
- [36] Abbaszadeh Sori A, Ebrahimnejad A, Motameni H. Elite artificial bees' colony algorithm to solve robot's fuzzy constrained routing problem. *Comput Intell* 2020;36(2):659–81. <https://doi.org/10.1111/COIN.12258>.
- [37] Di Caprio D, Ebrahimnejad A, Alrezaamiri H, Santos-Arteaga FJ. A novel ant colony algorithm for solving shortest path problems with fuzzy arc weights. *Alex Eng J* 2022;61(5):3403–15. <https://doi.org/10.1016/J.AEJ.2021.08.058>.
- [38] Awadallah MA, Al-Betar MA, Braik MS, Hammouri AI, Doush IA, Zitar RA. An enhanced binary rat swarm optimizer based on local-best concepts of PSO and collaborative crossover operators for feature selection. *Comput Biol Med* 2022;147:105675. <https://doi.org/10.1016/J.COMPBIOMED.2022.105675>.
- [39] Awadallah MA, Hammouri AI, Al-Betar MA, Braik MS, Elaziz MA. Binary horse herd optimization algorithm with crossover operators for feature selection. *Comput Biol Med* 2022;141:105152. <https://doi.org/10.1016/J.COMPBIOMED.2021.105152>.
- [40] Sayed GI, Soliman MM, Hassanien AE. A novel melanoma prediction model for imbalanced data using optimized SqueezeNet by bald eagle search optimization. *Comput Biol Med* 2021;136:104712. <https://doi.org/10.1016/J.COMPBIOMED.2021.104712>.
- [41] Chakraborty S, Saha AK, Nama S, Debnath S. COVID-19 X-ray image segmentation by modified whale optimization algorithm with population reduction. *Comput Biol Med* 2021;139:104984. <https://doi.org/10.1016/J.COMPBIOMED.2021.104984>.
- [42] Thawkar S, Sharma S, Khanna M, kumar Singh L. Breast cancer prediction using a hybrid method based on butterfly optimization algorithm and ant lion optimizer. *Comput Biol Med* 2021;139:104968. <https://doi.org/10.1016/J.COMPBIOMED.2021.104968>.
- [43] Emami SA, Poudeh MB, Eshtehardiha S. Particle swarm optimization for improved performance of PID controller on buck converter. In: Proceedings of the IEEE international conference on mechatronics and automation, ICMA 2008; 2008. p. 520–4. <https://doi.org/10.1109/ICMA.2008.4798810>.
- [44] Jalilvand A, Vahedi H, Bayat A. Optimal tuning of the PID controller for a buck converter using bacterial foraging algorithm. In: Proceedings of the international conference on intelligent and advanced systems, ICIAS 2010; 2010. <https://doi.org/10.1109/ICIAS.2010.5716105>.

- [45] Sonmez Y, Ayyildiz O, Kahraman HT, Guvenc U, Duman S. Improvement of buck converter performance using artificial bee colony optimized-PID controller. *J Autom Control Eng* 2015;3(4). Vol. 3vol. Vol.
- [46] Verma P, Patel N, Nair NKC, Sikander A. Design of PID controller using cuckoo search algorithm for buck-boost converter of LED driver circuit. In: Proceedings of the IEEE 2nd annual southern power electronics conference (SPEC), Auckland, New Zealand, IEEE; 2016. p. 1–4. <https://doi.org/10.1109/SPEC.2016.7846102>.
- [47] Wiangtong T, Sirapatcharangkul J. PID design optimization using flower pollination algorithm for a buck converter. In: Proceedings of the 17th international symposium on communications and information technologies (ISCIT); 2017. p. 1–4. <https://doi.org/10.1109/ISCIT.2017.8261202>.
- [48] Hekimoğlu B, Ekinci S. Optimally designed PID controller for a DC-DC buck converter via a hybrid whale optimization algorithm with simulated annealing. *Electrica* 2020;20(1):19–27. <https://doi.org/10.5152/ELECTRICA.2020.19034>.
- [49] Izci D, Hekimoğlu B, Ekinci S. A new artificial ecosystem-based optimization integrated with Nelder-Mead method for PID controller design of buck converter. *Alex Eng J* 2022;61(3):2030–44. <https://doi.org/10.1016/j.aej.2021.07.037>.
- [50] Mirjalili S. SCA: a sine cosine algorithm for solving optimization problems. *Knowl Based Syst* 2016;96:120–33. <https://doi.org/10.1016/j.knosys.2015.12.022>.
- [51] Abualigah L, Dulaimi AJ. A novel feature selection method for data mining tasks using hybrid sine cosine algorithm and genetic algorithm. *Clust Comput* 2021; 24(3):2161–76. <https://doi.org/10.1007/S10586-021-03254-Y>. 2021 24:3.
- [52] Li S, Chen H, Wang M, Heidari AA, Mirjalili S. Slime mould algorithm: a new method for stochastic optimization. *Future Gener Comput Syst* 2020;111:300–23. <https://doi.org/10.1016/j.future.2020.03.055>.
- [53] Su H, Zhao D, Heidari AA, Liu L, Zhang X, Mafarja M, Chen H. RIME: a physics-based optimization. *Neurocomputing* 2023;532:183–214. <https://doi.org/10.1016/j.neucom.2023.02.010>.
- [54] Heidari AA, Mirjalili S, Faris H, Aljarah I, Mafarja M, Chen H. Harris hawks optimization: algorithm and applications. *Future Gener Comput Syst* 2019;97: 849–72. <https://doi.org/10.1016/j.future.2019.02.028>.
- [55] Suid MH, Tumari MZM, Ahmad MA. A modified sine cosine algorithm for improving wind plant energy production. *Indones J Electr Eng Comput Sci* 2019;16(1): 101–6. <https://doi.org/10.11591/ijeecs.v16.i1.pp101-106>.
- [56] Gonidakis D, Vlachos A. A new sine cosine algorithm for economic and emission dispatch problems with price penalty factors. *J Inf Optim Sci* 2019;40(3): 679–97. <https://doi.org/10.1080/02522667.2018.1453667>.
- [57] Raut U, Mishra S. Power distribution network reconfiguration using an improved sine-cosine algorithm-based meta-heuristic search. *Adv Intell Syst Comput* 2019;816:1–13. https://doi.org/10.1007/978-981-13-1592-3_1.
- [58] Hekimoğlu B. Sine-cosine algorithm-based optimization for automatic voltage regulator system. *Trans Inst Meas Control* 2018;41. <https://doi.org/10.1177/0142331218811453>.
- [59] Nayak N, Mishra S, Sharma D, Sahu BK. Application of modified sine cosine algorithm to optimally design PID/fuzzy-PID controllers to deal with AGC issues in deregulated power system. *IET Gener Transm Distrib* 2019;13(12):2474–87. <https://doi.org/10.1049/IET-GTD.2018.6489>.
- [60] Abd Elfattah M, Abuelenin S, Hassanien AE, Pan JS. Handwritten Arabic manuscript image binarization using sine cosine optimization algorithm. *Adv Intell Syst Comput* 2016;536:273–80. https://doi.org/10.1007/978-3-319-48490-7_32.
- [61] Qian KF, Liu XT. Hybrid optimization strategy for lithium-ion battery's State of Charge/Health using joint of dual Kalman filter and modified sine-cosine algorithm. *J Energy Storage* 2021;44. <https://doi.org/10.1016/j.est.2021.103319>.
- [62] Gupta S, Deep K, Mirjalili S, Kim JH. A modified sine cosine algorithm with novel transition parameter and mutation operator for global optimization. *Expert Syst Appl* 2020;154. <https://doi.org/10.1016/j.eswa.2020.113395>.
- [63] Smedley K, Čuk S. Switching flow-graph nonlinear modeling technique. *IEEE Trans Power Electron* 1994;9(4):405–13. <https://doi.org/10.1109/63.318899>.